Artificial Hemoproteins

DOI: 10.1002/anie.200((will be filled in by the editorial staff))

Construction and Crystal Structure Analysis of Heme Acquisition Protein HasA Containing Iron(III)-5,15-Diphenylporphyrin and Derivatives Thereof as an Artificial Prosthetic Group**

*Hiromu Uehara†, Yuma Shisaka†, Tsubasa Nishimura, Hiroshi Sugimoto, Yoshitsugu Shiro, Yoshihiro Miyake, Hiroshi Shinokubo, Yoshihito Watanabe, and Osami Shoji**

Abstract: Iron(III)-5,15-diphenylporphyrin **(1)** and its derivatives **(2–7)** were accommodated by the heme acquisition protein HasA secreted by *Pseudomonas aeruginosa*, despite possessing bulky substituents at the meso-position of the porphyrin. Crystal structure analysis revealed that the two phenyl groups at the meso-positions of porphyrin extend outside HasA. It was shown that growth of *P. aeruginosa* was inhibited in the presence of HasA coordinating the synthetic porphyrins under iron-limiting conditions, and that the structure of the synthetic porphyrins greatly affects the inhibition efficiency.

Porphyrins are 18-π electron aromatic macrocycles that are composed of pyrrole subunits and found extensively in nature as heme and chlorophyll. Metalloporphyrins are involved in a wide variety of significant reactions in nature such as O_2 activation (cytochrome P450),[1] oxygen transport (hemoglobin),[2] and light-energy harvesting (light-harvesting antennae complex).[3]

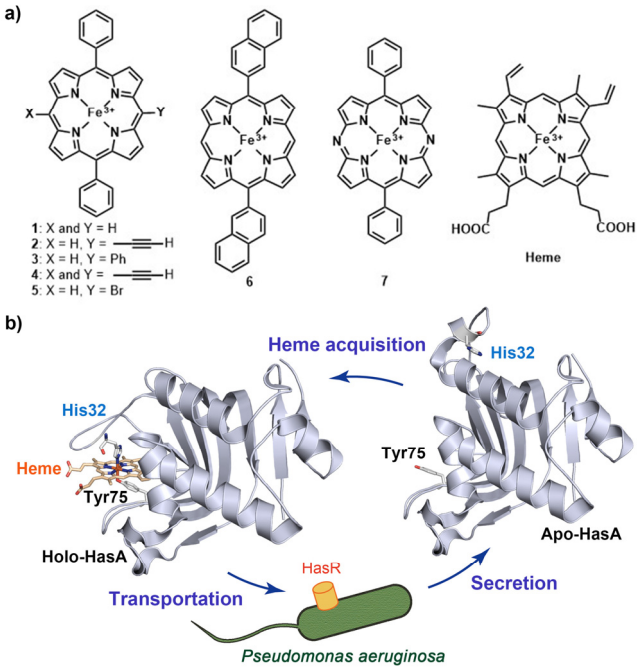

Figure 1. (a) The structures of Fe-DPP and its derivatives used in this study. (b) The heme acquisition system of *Pseudomonas aeruginosa*. Under low-iron conditions, *P. aeruginosa* secrets apo-HasA (PDB ID: 3MOK), which captures and transports heme (holo-HasA, PDB ID: 3ELL) to the outer membrane receptor HasR.

Given their biological importance, countless porphyrin derivatives with various structures have been prepared so that models of heme proteins can be constructed and bioinspired catalysts may be developed.[4] The function of heme proteins is dependent upon the properties of the heme molecule; thus, the reconstitution of heme proteins with synthetic porphyrins, such as protoporphyrin IX complexed with a metal other than iron, and heme molecules that are modified at the propionate groups, have been widely studied.[5] However, the incorporation of synthetic metal porphyrins with structures that differ from heme remains challenging, because most heme proteins accommodate heme with high selectively.

5,15-diphenylporphyrin (DPP) is a simple porphyrin that can be prepared by acid-catalyzed condensation of dipyrromethene with benzaldehyde in relatively good yield (25–40%),[6] and highly symmetric DPP derivatives with substitution at the meso and/or meso-phenyl group can also be prepared in reasonable yield.[7] The ease of access to DPP derivatives has prompted their use as building blocks for the construction of multi-

[*] Dr. O. Shoji, H. Uehara†, Y. Shisaka†
Department of Chemistry, Graduate School of Science, Nagoya University
Furo-cho, Chikusa-ku, Nagoya, 464-8602 (Japan)
Fax: (+81) 52-789-3557
E-mail: shoji.osami@a.mbox.nagoya-u.ac.jp
Homepage: http://bioinorg.chem.nagoya-u.ac.jp/
Dr. O. Shoji, H. Sugimoto
Core Research for Evolutional Science and Technology, Japan Science and Technology Agency, 5 Sanbancho, Chiyoda-ku, Tokyo, 102-0075 (Japan)
Prof. Dr. Y. Shiro
Guraduate School of Life Science, University of Hyogo, 3-2-1 Kouto, Sayo, Hyogo 678-1297 (Japan)
Dr. H. Sugimoto
RIKEN SPring-8 Center
1-1-1 Kouto, Sayo, Hyogo 679-5148 (Japan)
Prof. Dr. H. Shinokubo, Dr. Y. Miyake, T. Nishimura
Department of Molecular and Macromolecular Chemistry, Graduate School of Engineering, Nagoya University
Furo-cho, Chikusa-ku, Nagoya, 464-8603 (Japan)
Prof. Dr. Y. Watanabe
Research Center for Materials Science, Nagoya University
Furo-cho, Chikusa-ku, Nagoya, 464-8602 (Japan)

[†] These authors contributed equally to this work.

[**] This work was supported by Grant-in-Aid for Young Scientists (A) to O.S. (26708018) from the Ministry of Education, Culture, Sports, Science, and Technology (Japan) and JST CREST Grant Number JPMJCR15P3, Japan. This work was also supported by JSPS KAKENHI Grant Number JP15H05806 in Precisely Designed Catalysts with Customized Scaffolding to O. S.

Supporting information for this article is available on the WWW under http://www.angewandte.org.

porphyrin architectures[8] and catalysts.[9] However, neither DPP nor any of its derivatives have yet been complexed with natural heme proteins. Indeed, the incorporation of such compounds into natural heme proteins is expected to be difficult, because of the two bulky phenyl groups with perpendicular orientation to the porphyrin plane. However, there are reports that *de novo* designed peptides can accommodate DPP derivatives.[10] If it was possible to incorporate DPP or its derivatives into natural heme proteins, then these compounds could be used as synthetic prosthetic groups. It may thereby be possible to tune the biological function of heme proteins by changing the central metal ion and substituent groups. Herein, we report the first artificial metalloproteins incorporating Fe-DPP (**1**)[11] and its derivatives **2**–**7** by using the extracellular heme acquisition protein HasA secreted by *Pseudomonas aeruginosa* (Figure 1).

P. aeruginosa secretes HasA (apo-HasA)[12] under low-iron conditions to acquire heme as an iron source.[13] HasA captures heme and transports it to the specific receptor HasR, which is expressed in the outer membrane of *P. aeruginosa* (Figure 1b).[14] The heme is then taken up into cells via HasR where it is degraded for use as an iron source. The crystal structure of heme-bound HasA (holo-HasA) showed that the heme is coordinated by His32 and Tyr75, located in two independent loops, which hold the heme molecule in a manner akin to a pair of tweezers (Figure 1b).[15] The captured heme is highly exposed to the solvent, with three of the four pyrrole rings of heme accessible from outside the protein. This unique mode of heme binding in HasA suggested that it may be possible for this protein to accommodate DPP, including its two bulky phenyl groups at the meso-position, and we investigated whether HasA could indeed capture Fe-DPP (**1**). We also assessed the level of incorporation of several Fe-DPP derivatives **(2–6)** and iron(III)-5,15-diazaporphyrin **(7)**.[16] Given that growth of *P. aeruginosa* was shown to be inhibited in the presence of HasA coordinated to iron phthalocyanine (Fe–Pc),[17] we also investigated how the structure of the synthetic porphyrins captured by HasA affect the growth of *P. aeruginosa* under iron-limiting conditions. We envisaged that HasA containing suitably modified porphyrin derivatives could also serve as growth inhibitors.

We started our investigation by examining the complex formation of HasA with Fe-DPP (**1**). HasA without heme (apo-HasA) was added to a solution of **1** in DMSO. After removal of DMSO by dialysis, HasA with **1** was purified by anion-exchange column chromatography. The UV-Vis spectrum of the resulting brown solution showed absorption at 412 nm, which is assignable to the Soret absorption band of **1** (Figure 2a). ESI-TOF-MS analysis gave a peak with an *m*/*z* value corresponding to that of HasA complexed with **1**, and the ratio of peak intensity of the complex to that of apo-HasA was the same as that for the complex with heme-bound-HasA (Figures 2b and S1). Given that the ratio of peak intensity of apo-HasA to HasA with synthetic porphyrin reflects the stability of the complex,[18] HasA complexed with **1** appears to be as stable as heme-bound HasA. To further confirm the binding of **1** by HasA, a crystal structure of the complex of HasA with **1** was obtained at 2.0 Å resolution (Figure 2c). As was observed for heme-bound-HasA, the structure showed clear electron density for **1** at the heme-binding position, with both His32 and Tyr75 ligated to the iron of **1** (Figure 2d). The phenyl rings of **1** were accommodated in two distinct sites, one formed by His32(C=O), Pro34,

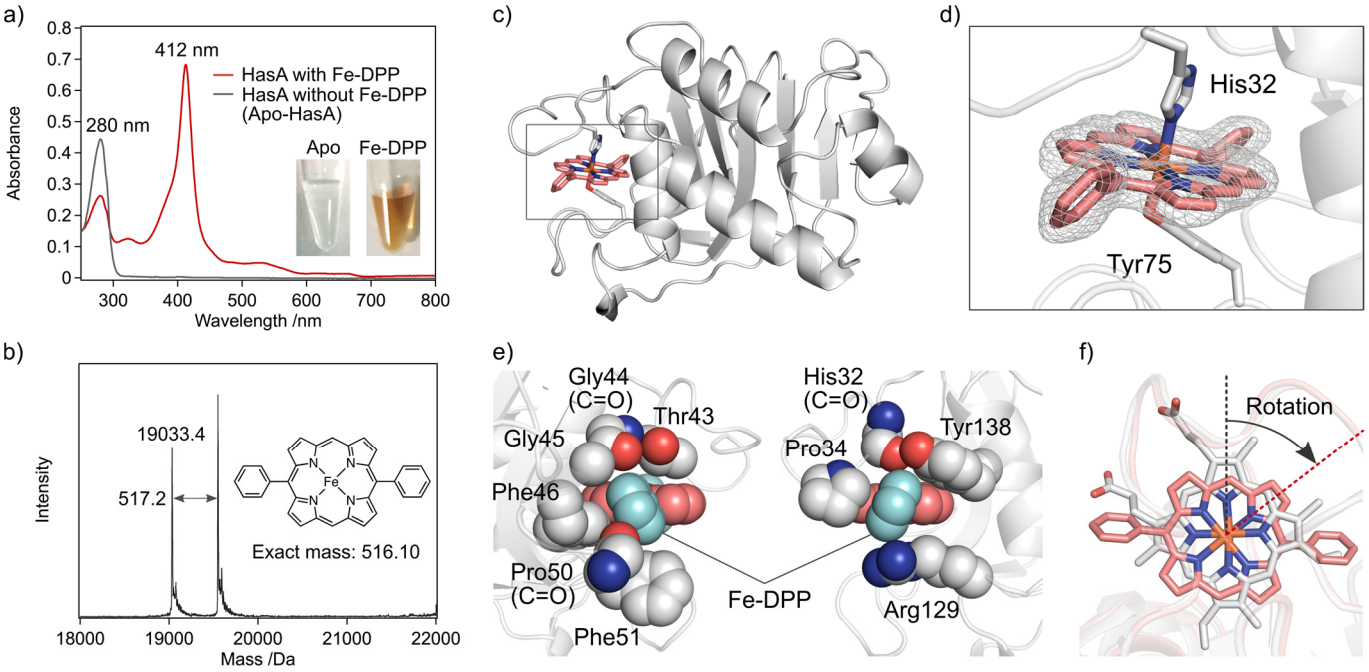

Figure 2. (a) UV-Visible spectra of HasA with Fe-DPP (**1**; red) and without Fe-DPP (apo-HasA; gray) in PBS solution. Protein solutions of apo-HasA and HasA with Fe-DPP (**1**) are shown in the inset. (b) ESI-TOF-MS spectrum of HasA with Fe-DPP (**1**) in 20 mM ammonium acetate buffer. (c)–(f) X-ray crystal structure of HasA incorporating Fe-DPP (**1**) (PDB ID: 5XIB): (c) Overall structure of HasA coordinating Fe-DPP (**1**) is indicated as pink sticks. (d) An enlarged view of the complex binding domain in HasA. The $2F_o$-F_c electron density map of Fe-DPP (**1**) contoured at the 1.0σ level is shown in gray mesh. (e) Side views of Fe-DPP (**1**) and the surrounding amino acids of HasA. The two phenyl groups at the meso-position of Fe-DPP (**1**) are shown in cyan. (f) Superimposition of HasA with Heme (PDB ID: 3ELL) and Fe-DPP (**1**). The angle of the porphyrin of Fe-DPP and heme differs by approximately 45° rotation. In all structures, oxygen, nitrogen, and iron are indicated in red, blue, and orange, respectively.

Arg129, and Tyr138, and the second site composed of Thr43, Gly44(C=O), Gly45, Phe46, Pro50(C=O), and Phe51 (Figure 2e). Interestingly, the porphyrin ring of **1** was rotated by approximately 45° with respect to the heme of holo-HasA (Figure 2f). This apparently serves to avoid steric crowding caused by the bulky phenyl groups at the meso-position. As evident from the crystal structure analysis, the overall structure of HasA ligating **1** is essentially identical to that of heme-bound HasA (root-mean-square deviation (RMSD) over 2–184 amino-acid residues for C_α atoms: 0.18), which indicates that structural perturbation upon binding of **1** is negligible.

Considering the stable complex formation between **1** and HasA, we examined Fe-DPP derivatives **2**–**7**, as shown in Figure 1a. ESI-TOF-MS analysis gave peaks corresponding to HasA complexed with **2**–**7,** although peaks for complexes of HasA with **3**[19] and **6** could only be detected in low amounts, suggesting that HasA does not form stable complexes with the latter derivatives (Figure S1). It was possible to crystallize HasA with **2**–**7** under similar conditions to those used to crystallize HasA with **1**, and crystal structures of HasA complexed with **2**, **3**, **4**, and **7** were obtained (Figure 3). In all cases, clear electron density of the DPP derivative was observed at the heme-binding site, with the overall structures being identical to that of heme-bound-HasA (Figures 3a, c, e, g, and S2). The angle of the porphyrin rings and the location of two phenyl rings were the same as for Fe-DPP (**1**) bound to HasA. The crystal structure of the complex with **2** showed that its ethynyl group was accommodated in the hydrophobic pocket, composed of Phe46, Tyr56, Leu85, His134, Val137, and Met141, located deep within the heme-binding site where, in the natural system, the vinyl group of heme is accommodated (Figures 3b and S3). In contrast to **2**, the phenyl ring at the 10-position of **3** was observed at the opposite side (outside of HasA) and exposed to the solvent (Figure 3d); the electron density of this phenyl group is partially disordered compared with the phenyl groups at the 5- and 15-positions, suggesting that the 10-phenyl is not so rigidly held, possibly due to the steric repulsion between the ring and the two loops of HasA, and particularly residues Val37 and Phe78 (Figure S4). This is consistent with the observation that ESI-TOF-MS analysis gave a weaker signal for HasA complexed with **3**, indicative of unstable binding. These results showed that the phenyl group at the 10-position of **3** is not accommodated in the hydrophobic pocket located in the heme-binding site because of its steric bulk. In fact, iron(III)-5,10,15,20-tetraphenylporphyrin (TPP) was not accommodated in HasA.[17] As evident from the crystal structure of HasA in complex with **4**, the ethynyl group can be located both inside and outside of the heme-binding site (Figure 3f). Notably, **7** was also accommodated by HasA even though the meso-carbon atoms were replaced by nitrogen atoms (Figure 3g, h). Crystal structure analysis revealed that HasA can accommodate Fe-DPP (**1**), **2**, **3**, **4**, and **7** without any structural perturbation (Figure S2).

Finally, we evaluated the inhibition activity of HasA with synthetic porphyrins **1**–**7**. We previously reported that iron phthalocyanine (Fe–Pc)–bound HasA markedly inhibits the growth of *P. aeruginosa* under iron-limiting conditions, even in the presence of heme-bound HasA (holo-HasA), which can provide heme as an iron source.[17] We reasoned that Fe–Pc bound HasA interacts strongly with its specific receptor, HasR, in the outer membrane of *P. aeruginosa*, resulting in inhibition of heme uptake via holo-HasA. Given that the overall structures of HasA containing synthetic porphyrins **1**–**7** are identical to that of holo-HasA, we expected that they could interact with HasR in the same manner as holo-HasA and inhibit heme acquisition through holo-HasA. In particular, we wished to establish whether differences in the structure of the synthetic metal complexes **1**–**7** affect the inhibition of *P. aeruginosa*, as overall structures of HasA containing synthetic porphyrins are identical irrespective of the structure of synthetic porphyrins (**1–4,** and **7**) examined in this research (Figure S2). Initially, HasA with porphyrin derivatives **1**–**7** were added to a culture solution of *P. aeruginosa* to examine whether the organism could utilize the synthetic porphyrins as a sole iron source. Under iron-limiting conditions *P. aeruginosa* did not grow, showing that it is not able to use synthetic porphyrins **1**–**7** as an iron source. Growth inhibition of *P. aeruginosa* in the presence of HasA complexed with

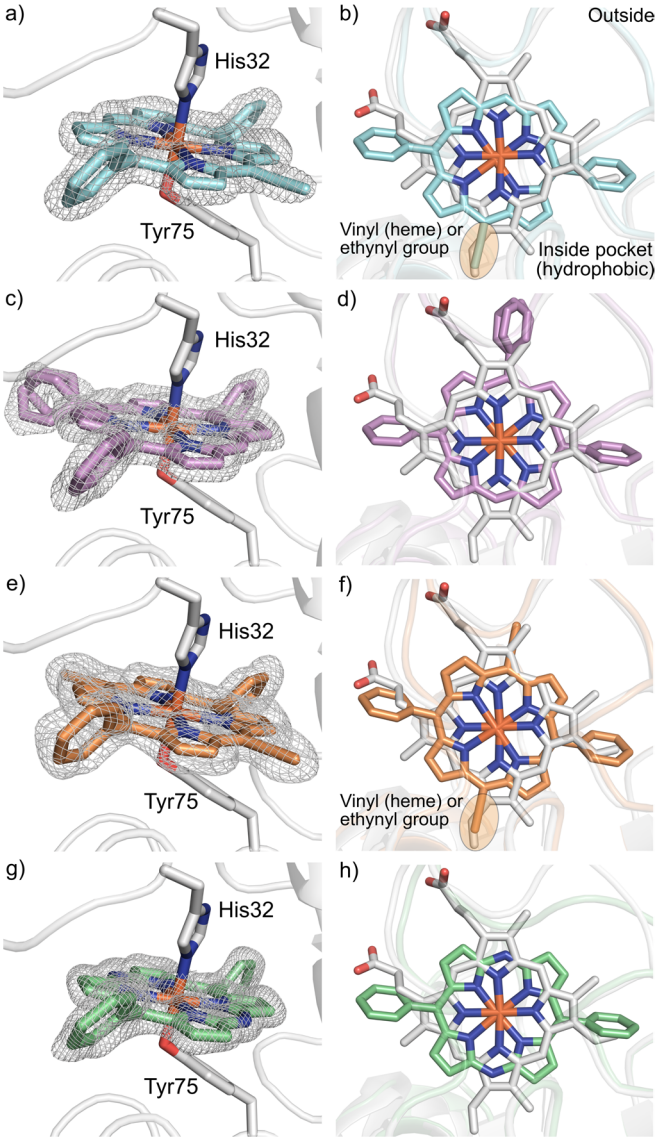

Figure 3. X-ray crystal structures of HasA with Fe-DPP derivatives: Fe-ethynylDPP (**2**; cyan; a, b; PDB ID: 5XIE); Fe-triPP (**3**; purple; c, d; PDB ID: 5XIC); Fe-bis(ethynyl)DPP (**4**; orange; e, f; PDB ID: 5XKB); and Fe-diazaDPP (**7**; green; g, h; PDB ID: 5XA4). (a, c, e, g) An enlarged view of complex binding domain in HasA. The $2F_o$-F_c electron density maps of each complex (**2**, **3**, **4**, and **7**) contoured at the 1.0σ level are shown as a gray mesh. (b, d, f, h) Superimposition of holo-HasA (white; PDB ID: 3ELL) and HasA coordinating Fe-DPP derivatives **2**, **3**, **4**, and **7**. The upper side of these figures corresponds to the outside, the opposite side of the hydrophobic pocket (inside). In all structures, oxygen and nitrogen are shown in red and blue, respectively.

porphyrins **1**–**7** was then examined. Accordingly, *P. aeruginosa* (PAO1) was first cultured in M9-based medium containing EDTA as an iron scavenger, and subsequent growth of the organism was monitored (absorption of the culture at 600 nm (OD_{600})) after the simultaneous addition of 1 μM of holo-HasA and 1 μM of HasA complexed with the synthetic porphyrins **1**–**7**. Growth inhibition of *P. aeruginosa* was observed for all HasA complexes. The efficacy of growth inhibition depended upon the structure of the porphyrin derivative employed (Figure 4a). Given that complexes of HasA with either **1** or **6** elicited weaker growth inhibition, further substitution at the meso-position of **1** with bromine, ethynyl, or phenyl groups was thought to be critical for efficient growth inhibition. Among the tested meso substituents, bromo- (**5**) and ethynyl (**2** and **4**) groups were found to be more suitable than a phenyl group at this position (**3**). Interestingly, use of complex **7** with HasA led to intense inhibition of *P. aeruginosa* growth. Given that we did not observe any clear difference in the overall fold of HasA between the porphyrins **1**–**7** (Figure S2), interactions between HasA and HasR are assumed to not differ significantly for this group. We assume that the synthetic porphyrins **1**–**7** are transported from HasA to HasR, whereupon they prevent the structural change of the receptor

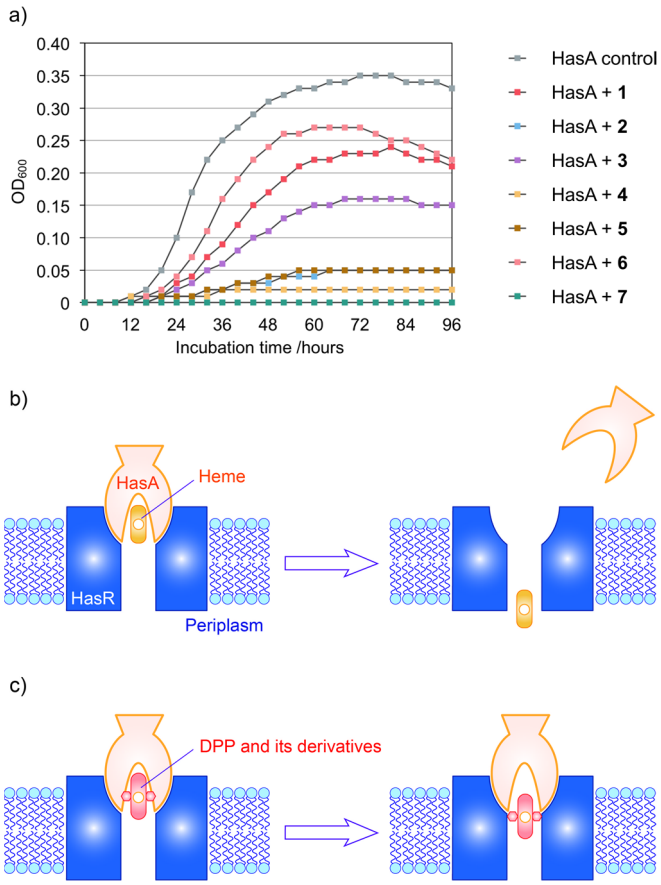

Figure 4. Growth inhibition of *P. aeruginosa* using artificial HasA under iron-limiting conditions. (a) Growth curve of *P. aeruginosa* in iron-limiting medium (M9-based medium). HasA control contained only 1 μM of HasA in complex with heme (holo-HasA) in the culture. In HasA with **1**–**7**, both 1 μM of holo-HasA and HasA in complex with synthetic porphyrins **1**–**7** were supplemented in the bacterial medium. (b) Transportation of the heme captured by HasA to HasR. After the heme transfer to HasR, HasA dissociates from HasR. (c) Proposed mechanism of growth inhibition of *P. aeruginosa* using HasA with Fe-DPP and its derivatives **1**–**7**. As a result of the steric repulsion of **1**–**7** with HasR, artificial HasA cannot dissociate from HasR and blocks heme transfer via holo-HasA.

HasR required for the release of apo-HasA. This blocking of the receptor hinders heme transfer from holo-HasA to HasR, resulting in growth inhibition (Figure 4b, c). Further studies are necessary to elucidate the mechanism governing the observed growth inhibition in more detail.

In conclusion, we have demonstrated that HasA secreted by *P. aeruginosa* can accommodate Fe-DPP (**1**) and its derivatives **2**–**7** without any structural perturbation. Crystal structure analysis revealed that two phenyl groups at the meso-position of the porphyrins extend outside of HasA to avoid steric crowding and are exposed to the solvent. To the best of our knowledge, this is the first example of a natural protein that stably binds Fe-DPP (**1**) and its derivatives **2**–**7**. Furthermore, we discovered that complexes of HasA with synthetic porphyrins inhibited the growth of *P. aeruginosa* under iron-limiting conditions. The structure of synthetic porphyrins greatly affected inhibition, with either substitution at the meso-position or replacement of meso-carbon atoms with nitrogen enhancing the inhibition efficiency. We concluded that the critical step governing inhibition is not interaction between HasA and HasR, but likely the interaction between HasR and the synthetic porphyrins transported from HasA to HasR. Although only a limited number of Fe-DPP derivatives have been examined herein for complex formation with HasA, further screening of synthetic porphyrins and/or combination with amino-acid replacement (mutagenesis) to alter the heme-binding site structure of HasA, based on the crystal structure of HasA reported in this study, would expand the range of synthetic porphyrins that can be accommodated by HasA. We envisage that HasA could be used as a host protein to accommodate various synthetic porphyrins to confer water solubility as well as to adjust the characteristics of the molecules such as electron potential and photophysical properties. Although we reported herein on growth inhibition, we believe that the combination of HasA with synthetic porphyrins can be used as prospective biocatalysts by tailoring the active site via mutagenesis for accommodation of substrates. Investigations along these lines are under way in our research group.

Received: ((will be filled in by the editorial staff))
Published online on ((will be filled in by the editorial staff))

Keywords: synthetic porphyrins · heme proteins · artificial HasA · protein structures · growth inhibition

[1] P. R. O. d. Montellano, *Cytochrome P450: Structure, Mechanism, and Biochemistry*, 4th ed., Plenum, New York, **2015**.
[2] Y. Yuan, M. F. Tam, V. Simplaceanu, C. Ho, *Chem. Rev.* **2015**, *115*, 1702-1724.
[3] a) Z. Liu, H. Yan, K. Wang, T. Kuang, J. Zhang, L. Gui, X. An, W. Chang, *Nature* **2004**, *428*, 287-292; b) G. McDermott, S. M. Prince, A. A. Freer, A. M. Hawthornthwaite-Lawless, M. Z. Papiz, R. J. Cogdell, N. W. Isaacs, *Nature* **1995**, *374*, 517-521.
[4] a) W. Liu, J. T. Groves, *Acc. Chem. Res.* **2015**, *48*, 1727-1735; b) S. Yoshikawa, A. Shimada, *Chem. Rev.* **2015**, *115*, 1936-1989; c) T. Higuchi, S. Uzu, M. Hirobe, *J. Am. Chem. Soc.* **1990**, *112*, 7051-7053; d) T. Yamane, K. Makino, N. Umezawa, N. Kato, T. Higuchi, *Angew. Chem. Int. Ed.* **2008**, *47*, 6438-6440.
[5] a) L. Fruk, C.-H. Kuo, E. Torres, C. M. Niemeyer, *Angew. Chem. Int. Ed.* **2009**, *48*, 1550-1574; b) K. Oohora, Y. Kihira, E. Mizohata, T. Inoue, T. Hayashi, *J. Am. Chem. Soc.* **2013**, *135*, 17282-17285; c) N. Kawakami, O. Shoji, Y. Watanabe, *ChemBioChem* **2012**, *13*, 2045-2047; d) E. W. Reynolds, M. W. McHenry, F. Cannac, J. G. Gober, C. D. Snow, E. M. Brustad, *J. Am. Chem. Soc.* **2016**, *138*, 12451-12458; e) H. M. Key, P. Dydio, D. S. Clark, J. F. Hartwig, *Nature* **2016**, *534*, 534-537; f) S.-C. Chien, O. Shoji, Y. Morimoto, Y. Watanabe, *New J. Chem.* **2017**, *41*, 302-307; g) M. B. Winter, E. J. McLaurin, S. Y. Reece, C. Olea, D. G. Nocera, M. A. Marletta, *J. Am. Chem. Soc.* **2010**, *132*, 5582-5583; h) T. Yonetani, T. Asakura, *J. Biol. Chem.* **1969**, *244*, 4580-4588; i) M. H. Gelb, W. A. Toscano, S. G. Sligar, *Proceedings of the National Academy of Sciences*

1982, *79*, 5758-5762; j) V. S. Lelyveld, E. Brustad, F. H. Arnold, A. Jasanoff, *J. Am. Chem. Soc.* **2011**, *133*, 649-651; k) R. Fasan, G. Sreenilayam, E. Moore, V. Steck, *Adv. Synth. Catal.* **2017**, *359*, 2076 – 2089; l) T. Hayashi, Y. Hisaeda, *Acc. Chem. Res.* **2002**, *35*, 35-43.

[6] C. Brückner, J. J. Posakony, C. K. Johnson, R. W. Boyle, B. R. James, D. Dolphin, *J. Porphyrins Phthalocyanines* **1998**, *02*, 455-465.

[7] S. Hiroto, Y. Miyake, H. Shinokubo, *Chem. Rev.* **2017**, *117*, 2910-3043.

[8] a) M. O. Senge, X. Feng, *Tetrahedron Lett.* **1999**, *40*, 4165-4168; b) T. Tanaka, A. Osuka, *Chem. Soc. Rev.* **2015**, *44*, 943-969; c) I. Beletskaya, V. S. Tyurin, A. Y. Tsivadze, R. Guilard, C. Stern, *Chem. Rev.* **2009**, *109*, 1659-1713.

[9] a) X. Jiang, F. Gou, F. Chen, H. Jing, *Green Chemistry* **2016**, *18*, 3567-3576; b) X. Jiang, F. Gou, H. Jing, *J. Catal.* **2014**, *313*, 159-167.

[10] a) F. V. Cochran, S. P. Wu, W. Wang, V. Nanda, J. G. Saven, M. J. Therien, W. F. DeGrado, *J. Am. Chem. Soc.* **2005**, *127*, 1346-1347; b) G. M. Bender, A. Lehmann, H. Zou, H. Cheng, H. C. Fry, D. Engel, M. J. Therien, J. K. Blasie, H. Roder, J. G. Saven, W. F. DeGrado, *J. Am. Chem. Soc.* **2007**, *129*, 10732-10740; c) I. V. Korendovych, A. Senes, Y. H. Kim, J. D. Lear, H. C. Fry, M. J. Therien, J. K. Blasie, F. A. Walker, W. F. DeGrado, *J. Am. Chem. Soc.* **2010**, *132*, 15516-15518; d) H. C. Fry, A. Lehmann, L. E. Sinks, I. Asselberghs, A. Tronin, V. Krishnan, J. K. Blasie, K. Clays, W. F. DeGrado, J. G. Saven, M. J. Therien, *J. Am. Chem. Soc.* **2013**, *135*, 13914-13926.

[11] L. Jaquinod, L. Prévot, J. Fischer, R. Weiss, *Inorg. Chem.* **1998**, *37*, 1142-1149.

[12] G. Jepkorir, J. C. Rodríguez, H. Rui, W. Im, S. Lovell, K. P. Battaile, A. Y. Alontaga, E. T. Yukl, P. Moënne-Loccoz, M. Rivera, *J. Am. Chem. Soc.* **2010**, *132*, 9857-9872.

[13] S. Létoffé, V. Redeker, C. Wandersman, *Mol. Microbiol.* **1998**, *28*, 1223-1234.

[14] S. Létoffé, C. Deniau, N. Wolff, E. Dassa, P. Delepelaire, A. Lecroisey, C. Wandersman, *Mol. Microbiol.* **2001**, *41*, 439-450.

[15] A. Y. Alontaga, J. C. Rodriguez, E. Schönbrunn, A. Becker, T. Funke, E. T. Yukl, T. Hayashi, J. Stobaugh, P. Moënne-Loccoz, M. Rivera, *Biochemistry* **2009**, *48*, 96-109.

[16] a) Y. Matano, T. Shibano, H. Nakano, Y. Kimura, H. Imahori, *Inorg. Chem.* **2012**, *51*, 12879-12890; b) Y. Matano, *Chem. Rev.* **2017**, *117*, 3138-3191.

[17] C. Shirataki, O. Shoji, M. Terada, S. Ozaki, H. Sugimoto, Y. Shiro, Y. Watanabe, *Angew. Chem. Int. Ed.* **2014**, *53*, 2862-2866.

[18] a) A. Kapur, J. L. Beck, S. E. Brown, N. E. Dixon, M. M. Sheil, *Protein Sci.* **2002**, *11*, 147-157; b) Y. Satake, S. Abe, S. Okazaki, N. Ban, T. Hikage, T. Ueno, H. Nakajima, A. Suzuki, T. Yamane, H. Nishiyama, Y. Watanabe, *Organometallics* **2007**, *26*, 4904-4908.

[19] J. Wojaczyński, L. Latos-Grażyński, P. J. Chmielewski, P. Van Calcar, A. L. Balch, *Inorg. Chem.* **1999**, *38*, 3040-3050.